

- 12, 196 (1979).
- 5) Bird, R. B., W. E. Stewart and E. N. Lightfoot: "Transport Phenomena", p. 668, Wiley, New York (1960).
 - 6) Cardner, D. V. and J. D. Hellums: *Ind. Eng. Chem., Fundam.*, **6**, 376 (1967).
 - 7) Clark, M. W. and C. J. King: *AIChE J.*, **16**, 64 (1970).
 - 8) Erickson, L. E., L. T. Fan and V. G. Fox: *Ind. Eng. Chem., Fundam.*, **5**, 19 (1966).
 - 9) Evans, H. L.: *Int. J. Heat Mass Transfer*, **3**, 321 (1961).
 - 10) Fox, V. G., L. E. Erickson and L. T. Fan: *AIChE J.*, **14**, 726 (1968).
 - 11) Hanna, O. T.: *ibid.*, **9**, 704 (1963).
 - 12) Hartnett, J. P. and E. R. G. Eckert: *Trans. ASME, Ser. C*, **79**, 247 (1957).
 - 13) Hirata, A.: *Kagaku Kōgaku*, **37**, 551 (1973).
 - 14) Hirata, A., K. Nagasawa and I. Koshijima: Preprint of the 41st Annual Meeting of The Soc. of Chem. Engrs., Japan, Sendai, D 303 (1976).
 - 15) Hirata, A., K. Kira and Y. Suzuki: *J. Chem. Eng. Japan*, **12**, 474 (1979).
 - 16) Merk, H. J.: *App. Sci. Res.*, **A-8**, 237 (1959).
 - 17) Nienow, A. W.: *Brit. Chem. Eng.*, **12**, 1737 (1967).
 - 18) Sadek, S. E.: *Ind. Eng. Chem., Fundam.*, **7**, 321 (1968).
 - 19) Shirotuka, T., A. Hirata and K. Sakai: *Kagaku Kōgaku*, **33**, 168 (1969).
 - 20) Shirotuka, T. and A. Hirata: *ibid.*, **34**, 904 (1970).
 - 21) Stewart, W. E.: *AIChE J.*, **8**, 421 (1962).
 - 22) *idem: ibid.*, **9**, 528 (1963).
 - 23) Stewart, W. E., J. B. Angelo and E. N. Lightfoot: *ibid.*, **16**, 771 (1970).
 - 24) Ueyama, K., J. Hatanaka and K. Ogawa: *J. Chem. Eng. Japan*, **5**, 371 (1972).

(Presented at the 12th Autumn Meeting of The Soc. of Chem. Engrs., Japan, at Okayama, 1978.)

EFFECT OF OSCILLATORY INSTABILITY ON STABILITY OF TWO-FLUID LAYERS

NOBUYUKI IMAISHI AND KATSUHIKO FUJINAWA
*Chemical Research Institute of Non-Aqueous Solutions,
 Tohoku University, Sendai 980*

TEIRIKI TADAKI
*Department of Chemical Engineering, Tohoku University,
 Sendai 980*

Condition for the onset of interfacial turbulence in mass transfer is investigated by a linear stability analysis. In a previous paper, it was revealed that inclusion of the Rayleigh effect as well as the Marangoni effect into analysis alters the stability limit and removes the contradiction between many experimental results and the Sternling and Scriven criteria of stability.

In this paper, the analysis is further extended to include oscillatory instability, which was neglected in the previous analysis.

The results show that oscillatory instability takes an important role in the onset of instabilities, and also that oscillatory instability always takes place when the destabilizing Rayleigh effect and the stabilizing Marangoni effect are competing.

It is suggested that the oscillatory instability of this kind may be correlated to the onset of violent interfacial turbulence or eruption.

Introduction

In a previous paper²⁾, it was revealed that the Rayleigh effect has a profound destabilizing influence upon Marangoni convection caused by interfacial mass transfer in horizontal two-fluid layers confined between two solid walls. In performing the analysis, however, it was assumed without proof that the marginal stability is stationary rather than oscillatory. This as-

sumption, referred to as the principle of exchange of stabilities, had been justified for the pure Rayleigh convection problem³⁾ and the pure Marangoni convection problems^{1,6)} of single-fluid layers. Sternling and Scriven⁵⁾, however, found that both stationary and oscillatory instabilities appear in the pure Marangoni convection problem in two-fluid layers.

In this paper, the same subject as ref. 2) is analysed again, without assuming the exchange of stabilities in order to assess the influence of oscillatory instability on the stability of two-fluid layers subjected to both the Rayleigh and the Marangoni effects in concert.

Received November 29, 1979. Correspondence concerning this article should be addressed to N. Imaishi.

1. Analysis

Consider two immiscible viscous fluids, as shown in Fig. 1 of ref. 2), bounded by horizontal solid surfaces of infinite extent held at constant concentrations. To test the stability of the two-fluid layers, use is made of the well-known linear stability analysis in each phase which, after linearization, reduces the equations in terms of the perturbation variables to

$$\nabla^2 \left\{ \frac{\partial}{\partial t} - \nu_j \nabla^2 \right\} w_j = -\frac{g}{\rho_j} \left(\frac{\partial \rho}{\partial C} \right)_j \nabla_{11}^2 \theta_j \quad (1)$$

and

$$\left\{ \frac{\partial}{\partial t} - D_j \nabla^2 \right\} \theta_j = -\beta_j \cdot w_j \quad (2)$$

where $\beta_j = (\partial C_j / \partial z)$ is the presumed initial linear concentration gradient. The boundary conditions are

$$\left. \begin{aligned} &\text{a) } \partial w_1 / \partial z = 0 \quad \text{b) } w_1 = 0 \quad \text{c) } \theta_1 = 0 \quad \text{at } z = d_1 \\ &\text{d) } \partial w_2 / \partial z = 0 \quad \text{e) } w_2 = 0 \quad \text{f) } \theta_2 = 0 \quad \text{at } z = -d_2, \\ &\text{and at } z = 0, \\ &\text{g) } \theta_1 = m \theta_2 \quad \text{h) } \beta_2 (\partial \theta_1 / \partial z) = \beta_1 (\partial \theta_2 / \partial z) \\ &\text{i) } w_1 = w_2 = 0 \quad \text{j) } \partial w_1 / \partial z = \partial w_2 / \partial z \\ &\text{k) } (\partial \sigma / \partial C_2) \nabla_{11}^2 \theta_2 = \mu_1 (\partial^2 w_1 / \partial z^2) - \mu_2 (\partial^2 w_2 / \partial z^2) \end{aligned} \right\} \quad (3)$$

This set of differential equations and boundary conditions defines an eigenvalue problem.

Eigenfunctions are assumed to have the form of

$$w_j = W_j(z) e^{i\alpha x} e^{\gamma t}, \quad \theta_j = \Theta_j(z) e^{i\alpha x} e^{\gamma t}$$

where α is wave number of the disturbance and γ is growth constant which is a complex variable in general, $\gamma = \gamma_R + i\gamma_I$. In the previous analysis, only the conditions for neutral stationary stability were investigated, thus the value of γ was always set to be zero.

The following nondimensional variables are introduced.

$$\begin{aligned} \bar{W}_j &= \frac{d_j}{\nu_j} W_j, & \bar{\Theta}_j &= \frac{D_j}{\beta_j d_j \nu_j} \Theta_j \\ \bar{z}_j &= \frac{z}{d_j}, & b_j &= d_j \alpha, & \bar{\gamma}_j &= \frac{d_j^2}{\nu_j} \gamma \end{aligned}$$

Equations (1)-(3) are reduced to

$$[(D_j^2 - b_j^2 - \bar{\gamma}_j)(D_j^2 - b_j^2 - Sc_j \cdot \bar{\gamma}_j)(D_j^2 - b_j^2) + b_j^2 \cdot Ra_j] \bar{W}_j = 0 \quad (4)$$

$$\left. \begin{aligned} &\text{a) } D_1 \bar{W}_1 = 0 \quad \text{b) } \bar{W}_1 = 0 \quad \text{c) } \bar{\Theta}_1 = 0 \quad \text{at } \bar{z}_1 = 1 \\ &\text{d) } D_2 \bar{W}_2 = 0 \quad \text{e) } \bar{W}_2 = 0 \quad \text{f) } \bar{\Theta}_2 = 0 \quad \text{at } \bar{z}_2 = -1 \\ &\text{and at } \bar{z}_1 = \bar{z}_2 = 0, \\ &\text{g) } \beta^* \nu^* \bar{\Theta}_1 = m D^* \bar{\Theta}_2 \quad \text{h) } \nu^* D_1 \bar{\Theta}_1 = D^* D_2 \bar{\Theta}_2 \\ &\text{i) } \bar{W}_1 = \bar{W}_2 = 0 \quad \text{j) } \nu^* D_1 \bar{W}_1 = r^2 D_2 \bar{W}_2 \\ &\text{k) } -b_2^2 Ma_2 \bar{\Theta}_2 = \nu^* \mu^* D_1^2 \bar{W}_1 / r^3 - D_2^2 \bar{W}_2 \end{aligned} \right\} \quad (5)$$

where

† In this analysis the effect of interfacial contamination is not taken into account.

Table 1 Summary of property ratios

Solute	D^*	ν^*	μ^*	Δ^*	m	Sc_2	β^*
Acetic acid	1.957	0.6914	0.604	0.5649	0.0143	1140	$1/D^*$
Acetone	1.953	0.6914	0.604	0.6542	0.8511	830	$1/D^*$

Solvents: Benzene (phase 1) and Water (phase 2)

$$\bar{\Theta}_j = -(D_j^2 - b_j^2 - \bar{\gamma}_j)(D_j^2 - b_j^2) \bar{W}_j / (b_j^2 \cdot Ra_j) \quad (6)$$

$$\mu^* = \mu_1 / \mu_2, \quad \nu^* = \nu_1 / \nu_2, \quad D^* = D_1 / D_2, \quad \beta^* = \beta_1 / \beta_2$$

$$r = d_1 / d_2$$

and $D_j^2 = d^n / d\bar{z}_j^n$. Ra_j and Ma_j are the Rayleigh and the Marangoni numbers in the j -th phase respectively. The general solution to Eq. (4) is

$$\bar{W}_j = \sum_{i=1}^6 a_{ij} \cdot e^{n_i j \bar{z}_j} \quad (7)$$

where n_{ij} is the i -th root of the characteristic equation for the Eq. (4).

Substitution of Eq. (7) into Eqs. (5) through (6) yields twelve linear homogeneous algebraic equations for the twelve unknown constants a_{ij} . For the solutions to be nontrivial, the characteristic determinant of the coefficient matrix must vanish.

$$H(b_j, Ra_j, Ma_2, r, D^*, \nu^*, \beta^*, \mu^*, m, Sc_j, \bar{\gamma}_j) = 0 \quad (8)$$

For a pair of fluids, D^* , ν^* , β^* , μ^* , $\rho^* = \rho_1 / \rho_2$ and $\Delta^* = (\rho_2 / \rho_1)(\partial \rho / \partial C)_1 / (\partial \rho / \partial C)_2$ are all specified. The values of b_1 , b_2 , Sc_1 , Sc_2 and Ra_1 , Ra_2 are related to each other by the following equations.

$$b_1 = r b_2, \quad Ra_1 = (\Delta^* \beta^* r^4 / \nu^* D^*) Ra_2, \quad Sc_1 = (\nu^* / D^*) Sc_2$$

Hence, for a given system, the relation between Ma_2 and b_2 for an arbitrary value of Ra_2 is calculated from Eq. (8). For a given complex value of $\bar{\gamma}_2$, the calculation will generally result in a complex value of Ma_2 . The result, however, has a physical significance only when the imaginary part of Ma_2 is zero. A digital computer program was written to find automatically the values of $\bar{\gamma}_{2I}$ which correspond to the points where the imaginary part of Ma_2 vanishes, for an arbitrary value of $\bar{\gamma}_{2R}$.

2. Numerical Results and Discussion

2.1 Specific results

At first, calculated results for two particular cases are described.

Calculations were made for the benzene-water two-fluid layer in which acetic acid or acetone is transferred through the interface. These systems are chosen with particular reference to make a comparison between the present results and the previous work²⁾. The ratios of physical properties used in the calculations are listed in Table 1.

1) Acetic acid ($r=1.0$) The Marangoni number corresponding to the marginal stabilities ($\bar{\gamma}_{2R}=0$) are

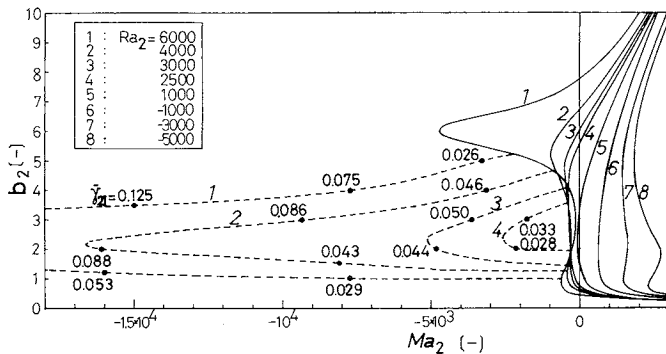


Fig. 1 Marginally stable Marangoni number as a function of wave number for various Rayleigh numbers for transfer of acetic acid

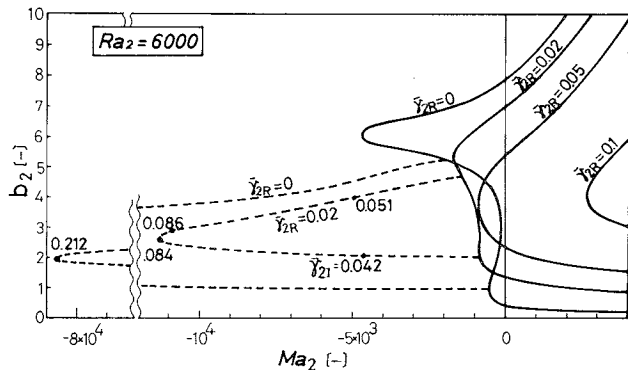


Fig. 2 Relationship between the Marangoni number and wave number for the marginally stable and growing disturbance (acetic acid, $Ra_2=6000$)

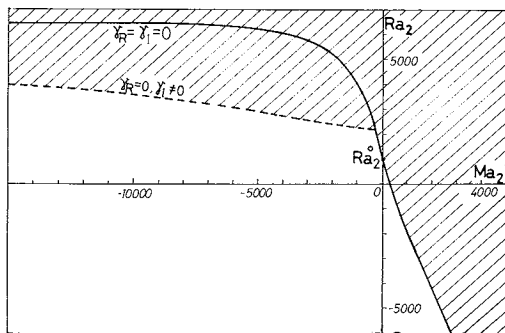


Fig. 3 Stability diagram for transfer of acetic acid

shown in Fig. 1 as a function of the wave number. For a given value of the Rayleigh number, the region to the left of each curve corresponds to the stable state, whereas for the right of the curve the system is unstable. Solid lines denote the stationary marginal (neutral) state ($\bar{\gamma}_2 = \bar{\gamma}_{2R} = \bar{\gamma}_{2I} = 0$), and the dotted lines the oscillatory marginal state ($\bar{\gamma}_{2R} = 0$ but $\bar{\gamma}_{2I} \neq 0$). In this system, the oscillatory marginal state appears only when the Rayleigh number Ra_2 exceeds 2100. The behaviour of the oscillatory instability is elucidated in Fig. 2 for the case of $Ra_2=6000$. In the figure, the Ma_2 - b_2 relations are plotted not only for marginal state but also for growing instabilities ($\bar{\gamma}_{2R} > 0$). As $\bar{\gamma}_{2R}$ increases, oscillatory instability prevails in nar-

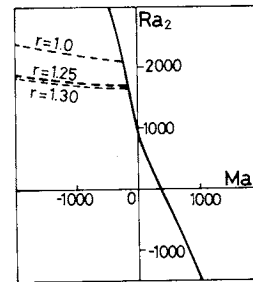


Fig. 4 Response of oscillatory instability curve for liquid depth ratios for transfer of acetic acid

rower region. And when $\bar{\gamma}_{2R}$ exceeds 0.05, no oscillatory instability appears.

The stability diagram is obtained as shown in Fig. 3. The hatched region denotes unstable state. The solid line in Fig. 3 corresponds to stationary neutral state. This line is the same as that of the previous work. The dotted line corresponds to oscillatory neutral state. This diagram shows that the assumption of the principle of exchange of stabilities misleads to too wide a stable region when the direction of mass transfer is from benzene to water; that corresponds to the second quadrant of the stability diagram.

2) Acetone ($r=1.0$) The stability diagram for this system is similar to that shown in Fig. 3. Oscillatory instability is predicted only in the 2nd quadrant of the diagram ($Ra_2 > 0, Ma_2 < 0$). For this system, however, only the 1st and 3rd quadrants of the diagram have respective physical significance (see ref. 2)). Therefore the oscillatory instability exerts no influence on the stability criterion. Figure 5 of ref. 2) can be used with no correction.

3) Response to the liquid depth ratio r . In these two cases, the liquid depth ratio r is revealed to exert a small influence on the incipience of oscillatory instability. Increasing the value of r shifts the stability curve corresponding to oscillatory instability downward on the stability diagram to a small extent, as shown in Fig. 4. Further increase in r results in the appearance of the other mode of stationary instability, as shown in Figs. 6 and 7 of ref. 2). In such a case, oscillatory instability is no longer responsible for the stability of the system.

2.2 Miscellaneous results

Some calculations other than for the above two systems were conducted to explain the influence of oscillatory instability on two-fluid Rayleigh-Marangoni problem more generally. Table 2 shows the combinations of property ratios used. Sterling and Scriven⁵⁾ showed that the pure Marangoni instability in a two-fluid layer of infinite depth is classified into 10 modes in accordance with the order of D^* , ν^* (r^2 and e^2 in ref.

Table 2 Summary of property ratios

Case	D^*	ν^*	μ^*	Δ^*	m	Sc_2	β^*	
1	1.957	0.6914	0.604	0.5649	0.0143	1140	$1/D^*$	$D^* > 1 > \nu^*, f > 0$
2	1.957	0.6914	0.604	0.5649	0.0143	10	$1/D^*$	$D^* > 1 > \nu^*, f > 0$
3	0.500	0.8000	0.604	0.5649	0.0143	700	$1/D^*$	$1 > \nu^* > D^*, f > 0$
4	1.953	0.2000	0.180	0.6350	0.8511	830	$1/D^*$	$D^* > 1 > \nu^*, f > 0$
5	1.957	1.2000	0.604	0.9815	0.0143	1140	$1/D^*$	$D^* > \nu^* > 1, f > 0$
6	1.000	0.6914	0.604	0.6542	0.8511	830	$1/D^*$	$D^* = 1 > \nu^*, f > 0$
7	1.200	0.6914	0.604	-1.1440	1.0000	800	$1/D^*$	$D^* > 1 > \nu^*, f > 0$

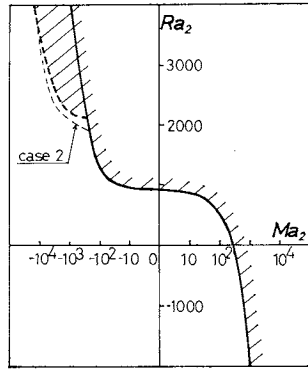


Fig. 5 Stability diagrams for Case 1 and Case 2

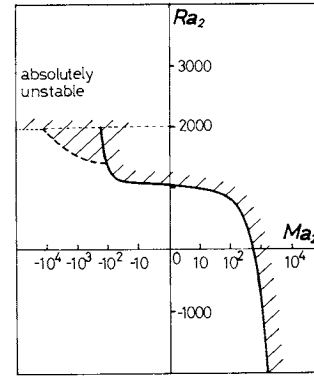


Fig. 7 Stability diagram for Case 4

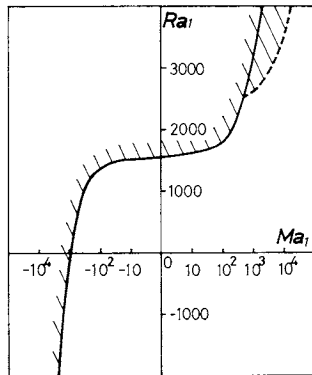


Fig. 6 Stability diagram for Case 3

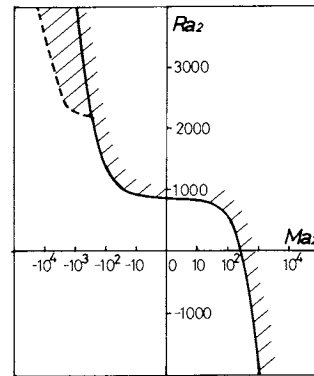


Fig. 8 Stability diagram for Case 5

5)) and also with the sign of a parameter f (for the definition of f , see Eq. (34) of ref. 5)). The last column of Table 2 shows the order of these parameters for ready comparison.

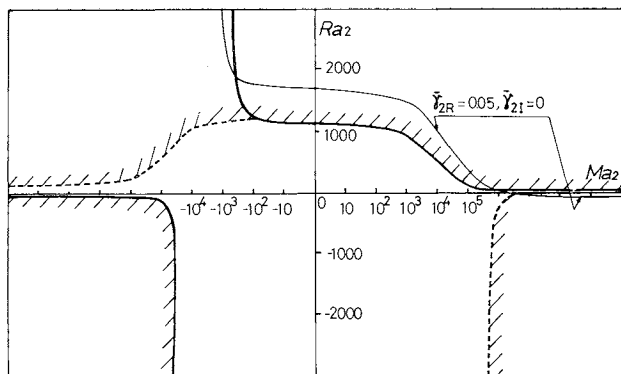
Resulting stability diagrams are shown in Figs. 5 through 10. In these figures, an unusual coordinate scaling is employed for clarity of presentation.

Case 1 corresponds to the above-mentioned water-(acetic acid)-benzene system. Case 2 is chosen to examine the effect of Sc_2 . Since stationary neutral stability is independent of Sc_2 , the effect of Sc_2 is exerted only on oscillatory neutral instability. As shown in Fig. 5, its effect is revealed to be less significant. Figure 6 shows the stability diagram for a system in which D^* is smaller than unity. If D^* is smaller than unity, the stability diagram obtained is a mirror image of that of a system in which D^* is greater than unity. In Fig. 6, the stability diagram is represented

in terms of Ra_1 and Ma_1 , since they are greater than Ra_2 and Ma_2 in this system.

All of these results show that the inclusion of oscillatory instability in analysis results in predicting a narrower stable region and that a careless use of the principle of exchange of stabilities may cause serious error in many cases.

The results of these numerical studies, however, cannot justify the setting up of such a general criterion for the incipience of oscillatory instability as that shown by Sternling and Scriven for the pure Marangoni instability in two-fluid layer of infinite depth. The three stability parameters of Sternling and Scriven, D^* , ν^* and f are revealed to be no longer responsible in predicting the incipience of the purely Marangoni effect-induced oscillatory instability in a two-fluid layer of finite depth, except in case 6. The upper and lower solid walls stabilize the fluid layer against oscillatory insta-



On the Ma_2 axis, there is no stationary marginal state, though there exists growing stationary instability, if $Ma_2 \gg 0$.

Fig. 9 Stability diagram for Case 6

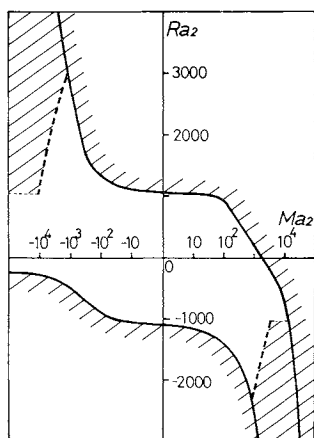


Fig. 10 Stability diagram for Case 7

bility with increasing viscous dissipation.

When a vigorously destabilizing Rayleigh effect is imposed, all of these systems first become unstable with oscillatory instability. The origin of this oscillatory instability is explained in terms of a competition of the two counteracting driving mechanisms. When Ra_j exceeds Ra_j^* , the Rayleigh effect provokes the fluid into motion. But if the fluid begins to move, the Marangoni effect takes place to prevent the motion. Consequently, a to-and-fro fluid motion may be originated; this motion corresponds to the oscillatory instability in this case. If Δ^* is negative as in case 7, oscillatory instability of this type can occur in two quadrants in the stability diagram, Fig. 10.

2.3 Discussion

It may be worthwhile to consider to what phenomena the mathematically predicted oscillatory instability does correspond, although the authors well recognize that the linear stability analysis deals only with infinitesimal disturbances which cannot be compared with the observable disturbances, and that the shortcomings in the model cause certain limitations on its predictions.

In the other field of stability problems, the oscil-

latory instability corresponds to the origin of the turbulence, as the origin of the turbulent flow, whereas the stationary instabilities often correspond to the ordered roll cell convections, the Taylor instability and the well-known Benard cells.

It is well-known that a vigorous turbulence characterized by the existence of localized dilation-compression movements, eruption, is provoked by the interfacial mass transfer of acetic acid from benzene to water. In the reverse direction of transfer, on the contrary, only a slow and gentle fluid motion is produced. This fact and the stability diagram of Fig. 3 suggest that the oscillatory instability is closely connected to the incipience of interfacial turbulence. It coincides with Sawistowski's explanation of the origin of eruption⁴). If it is so, the incipience of interfacial turbulence is successfully predicted by this linear stability analysis in which both the Rayleigh and the Marangoni effects and also the oscillatory instability are all taken into account. As it is, however, the relation between oscillatory instability and the incipience of interfacial turbulence is not yet rigorously assured and should be further confirmed in other liquid-liquid mass transfer systems.

Conclusion

The previously reported linear stability analysis of two-fluid layers is extended to include oscillatory instability. It is revealed that oscillatory instability takes place whenever the vigorously destabilizing Rayleigh effect and the counteracting Marangoni effect are competing.

Incipience of oscillatory instability is often responsible for the destabilization of the fluid layers. Therefore, in order to predict correctly the stability limit of two-fluid layers, in which both the Rayleigh and the Marangoni effects prevails, oscillatory instability should be always taken into account.

Nomenclature

b_j	= nondimensional wave number	[—]
C_j^0	= initial concentration distribution	[mol/m ³]
D_j	= differential operator (=d/d \bar{z}_j)	[—]
D	= diffusivity	[m ² /s]
d	= liquid depth	[m]
g	= gravitational acceleration constant	[m/s ²]
i	= $\sqrt{-1}$	[—]
Ma	= Marangoni number (= $\beta(\partial\sigma/\partial C)d^2/\mu D$)	[—]
m	= distribution coefficient (= C_1/C_2)	[—]
Ra	= Rayleigh number (= $-\beta \cdot \Delta \cdot g \cdot d^4/\nu D$)	[—]
r	= liquid depth ratio (= d_1/d_2)	[—]
t	= time	[s]
W	= eigenfunction of velocity perturbation	[m/s]
w	= z component of velocity	[m/s]
x	= coordinate	[m]
z	= coordinate	[m]
α	= wave number	[1/m]

β	= presumed initial concentration gradient	[mol/m ⁴]
γ	= growth constant	[1/s]
Δ	= expansion coefficient ($= -(\partial\rho/\partial C)_j/\rho_j$)	[m ³ /mol]
Θ	= eigenfunction of concentration perturbation	[mol/m ³]
θ	= concentration perturbation	[mol/m ³]
μ	= viscosity	[N·s/m ²]
ρ	= density	[kg/m ³]
σ	= interfacial tension	[N/m]
∇^2	= $\partial^2/\partial x^2 + \partial^2/\partial y^2 + \partial^2/\partial z^2$	
∇_{II}^2	= $\partial^2/\partial x^2 + \partial^2/\partial y^2$	
<Subscripts>		
I	= imaginary part of complex value	
j	= ($j=1, 2$) phase 1 (the upper fluid layer) and phase 2 (the lower fluid layer)	
R	= real part of complex value	

<Superscripts>

-	= nondimensional form
*	= ratio (property of phase 1/ property of phase 2)

Literature Cited

- 1) Brian, P.L.T. and K. A. Smith: *AIChE J.*, **18**, 231 (1972).
- 2) Imaishi, N. and K. Fujinawa: *J. Chem. Eng. Japan*, **7**, 81 (1974).
- 3) Pellew, A. and R. V. Southwell: *Proc. Roy. Soc. London, Ser. A*, **176**, 312 (1940).
- 4) Sawistowski, H.: 'Interfacial Phenomena' in "Recent Advances in Liquid-Liquid Extraction", ed. C. Hanson, Pergamon Press, 1971.
- 5) Sternling, C. V. and L. E. Scriven: *AIChE J.*, **5**, 514 (1959).
- 6) Vidal, A. and A. Acrivos: *Phys. Fluids*, **9**, 615 (1966).

AXIAL MIXING OF PARTICLES IN ROTARY DRYERS AND COOLERS

HIDEHARU HIROSUE

Government Industrial Research Institute, Kyushu,
Tosu 841

For the purpose of making clear the mechanism involved in the axial mixing of particles in rotary dryers and coolers, the axial mixing of particles in batch systems was measured.

The diffusion model has been applied to the axial mixing of particles in batch and continuous systems and the influence of the operating variables on the diffusion coefficient in batch systems and on the axial dispersion coefficient in continuous systems has been examined.

As a result, it is found that the influence of the operating variables on both the coefficients is essentially the same and that the ratio of diffusion coefficient to axial dispersion coefficient is approximately equal to 0.7 under the same experimental conditions. This result indicates that as the axial mixing of particles in the batch system is considered to be due to collision and bounce between the particles falling from the flights and the bare wall, the lifting flights and the particles deposited in the lower part of the dryer collision and bounce may be a major mechanism involved in the axial mixing of particles in continuous rotary dryers and coolers.

Introduction

The residence time distribution of particles is of importance for the design and performance of rotary dryers and coolers because it is directly related to the nonuniformity of product quality.

It has therefore been already examined by some researchers^{4,9,11}) and the following results were presented⁴):

1) The residence time distribution of particles in rotary dryers and coolers approximated to the logarithmic normal distribution, which has two parameters,

i. e. the geometric mean retention time and the geometric standard deviation.

2) The geometric mean retention time was nearly equal to the apparent mean retention time possible to estimate¹²). The experimental equations for the geometric standard deviation were obtained under conditions of both no air flow and air flow.

It was also found that the values of the geometric standard deviation were less than 0.1 whether there was air flow or not. This result suggests that the influence of the residence time distribution on the properties of the products may not be of importance.

However, for the purpose of making clear the

Received November 30, 1979.